

Spectral Energy and Age Distributions for 51 Globular Cluster Candidates

Jun Ma¹, Xu Zhou¹, Jiansheng Chen¹, Hong Wu¹, Xu Kong², Zhaoji Jiang¹, Jin Zhu¹, and Suijian Xue¹

ABSTRACT

This paper is the fourth in a series presenting spectrophotometry of 51 globular cluster candidates, that were detected by Mochejska et al. in the nearby galaxy M33 using the data collected by the DIRECT project. The frames of M33 in this study were taken as part of the BATC Multicolor Sky Survey. We obtained the spectral energy distributions of these candidates in 13 intermediate-band filters. By comparing the integrated photometric measurements with theoretical stellar population synthesis models of Bruzual & Charlot, we estimated their ages. The BC96 models provide the evolution in time of the spectrophotometric properties of simple stellar populations for a wide range of stellar metallicity. Our results show that half of the candidates are younger than 10^8 years, whose age degeneracy is not pronounced. We also find that globular clusters formed continuously in M33 from $\sim 4 \times 10^6 - 10^{10}$ years. Our results are in agreement with Chandar et al., who estimated ages for 35 globular clusters candidates in common by comparing the photometric measurements to integrated colors from theoretical models by Bertelli et al. The Kolmogorov-Smirnov Test shows that the maximum value of the absolute difference of estimated ages between Chandar et al. and us is 0.48, and the significance level probability is 100.00 per cent.

Subject headings: galaxies: individual (M33) – galaxies: evolution – galaxies: globular cluster candidates

1. INTRODUCTION

The Galactic globular clusters, which are thought to be among the oldest radiant objects in the universe and can be accurately dated in the Galaxy, provide vitally important information regarding the minimum age of the universe and the early formation history of our Galaxy. The study of these systems has contributed much to our knowledge of stellar evolution and galactic structure. However, it is necessary to make sure that the conclusions drawn from the study of the Milky Way’s globular cluster system are not biased either because they are somehow unusual or because our location in the Milky Way prevents us from fully characterizing its properties. So, the study of globular clusters in other galaxies is valuable, especially in Local Group galaxies. Besides the Milky Way, a few of other Local Group galaxies contain globular clusters, such as the Sagittarius dwarf spheroidal galaxy, the Large and Small Magellanic Clouds, M31, and M33. Christian & Schommer (1982, 1988) cataloged more than 250 non-stellar sources by visually examining 14×14 inch² unfiltered, unbaked, IIa-O focus plate of M33, and obtained ground based *BVI* photometry for ~ 106 star cluster candidates, and estimated that M33 contains only ~ 20 total “true” globular clusters. Using the *Hubble Space Telescope* WFPC2 multiband images of 55 fields in M33, Chandar, Bianchi, & Ford (1999a, 2001) detected 162 star clusters, 131 of which were previously unknown. They estimated the total number of globular clusters in M33 to be 75 ± 14 . Especially, Mochejska et al. (1998) detected 51 globular cluster candidates in M33, 32 of which were not previously cataloged, using the data collected in the DIRECT project (Kaluzny et al. 1998; Stanek et al. 1998).

¹National Astronomical Observatories, Chinese Academy of Sciences, Beijing, 100012, P. R. China; majun@vega.bac.pku.edu.cn

²Center for Astrophysics, University of Science and Technology of China, Hefei, 230026, P. R. China

M33 is a small Scd Local Group galaxy, about 15 times farther from us than the LMC (distance modulus is 24.64) (Freedman, Wilson, & Madore 1991; Chandar, Bianchi, & Ford 1999a). It is interesting and important because it represents a morphological type intermediate between the largest “early-type” spirals and the dwarf irregulars in the Local Group (Chandar, Bianchi, & Ford 1999a). At a distance of ~ 840 kpc, M33 is the only nearby late-type spiral galaxy, it can provide an important link between the cluster populations of earlier-type spirals (Milky Way galaxy and M31) and the numerous, nearby later-type dwarf galaxies. Our collaboration, the Beijing-Arizona-Taiwan-Connecticut (BATC) Multicolor Sky Survey (Fan et al. 1997; Zheng et al. 1999), already had M33 spiral galaxy as part of its galaxy calibration program.

Sarajedini et al. (1998) selected ten halo globular clusters from Schommer et al. (1991) by inspecting the difference between the cluster velocity and the disk velocity as a function of the integrated cluster color, and constructed color-magnitude diagrams to estimate the cluster metallicity using the shape and color of the red giant branch. Under the assumption that cluster age is the global second parameter, Sarajedini et al. (1998) presented that the average age of halo globular clusters in M33 appears to be a few Gyrs younger than halo clusters in the Milky Way. Ma et al. (2002a) also estimated their ages by comparing the photometry of each object with theoretical stellar population synthesis models for different values of metallicity, and the results showed that eight clusters have “intermediate” ages, i.e. between 1 and 8 Gyrs.

In this paper, we present the SEDs of 37 globular cluster candidates that were detected by Mochejska et al (1998) in M33, and age estimates for these candidates by comparing the integrated photometric measurements with theoretical stellar population synthesis models. The multi-color photometry is powerful to provide the accurate SEDs for these stellar clusters.

The outline of the paper is as follows. Details of observations and data reduction are given in section 2. In section 3, we provide a brief description of the stellar population synthesis models of Bruzual & Charlot (1996, unpublished, hereafter BC96). The distributions of metallicity and age are given in section 4. The summary and discussion are presented in section 5.

2. SAMPLE, OBSERVATIONS AND DATA REDUCTION

2.1. Sample of Globular Cluster Candidates

The sample in this paper is from Mochejska et al. (1998), who detected 51 globular cluster candidates using the data collected in the DIRECT project (Kaluzny et al. 1998; Stanek et al. 1998). In this project, the observations for M33 were done with the 1.2 m telescope at the F. L. Whipple Observatory, using a thinned, back-side illuminated, AR-coated Loral 2048 \times 2048 CCD. The pixel scale is $0''.3$. Mochejska et al. (1998) also presented the photometry for these candidates using standard Johnson-Cousins *BVI* filters. Although searching for star clusters in M33 is sporadic, this work has been continued (Hiltner 1960; Kron & Mayall 1960; Melnick & D’Odorico 1978; Christian & Schommer 1982, 1988; Mochejska et al. 1998; Chandar, Bianchi, & Ford 1999a, 2001). 19 of the 51 globular cluster candidates in Mochejska et al. (1998) were previously detected by Melnick & D’Odorico (1978) or Christian & Schommer (1982). Table 2 summarizes the common clusters in different studies. The clusters with symbol (*) were also studied by Ma et al. (2001, 2002a, 2002b), who presented their SEDs in 13 intermediate band filters, and age estimates by comparing the photometry of each object with theoretical stellar population synthesis models for different values of metallicity. In this study, we will present the SEDs and age estimates for 37 globular cluster candidates that were not found in Ma et al. (2001, 2002a, 2002b). However, we will plot the age distribution of the 51 candidates for obtaining the whole picture of these globular clusters formation. Figure 1 is the image of M33 in filter BATC07 (5785Å), the circles and the numbers in which indicate the positions and names of the 51 globular cluster candidates.

Fig. 1.— The image of M33 in filter BATC07 (5785Å) and the positions of the sample globular cluster candidates. The center of the image is located at R.A. = $01^{\text{h}}33^{\text{m}}50^{\text{s}}.58$, decl. = $30^{\circ}39'08''.4$ (J2000.0). North is up and east is to the left.

2.2. CCD Image Observation

The large field multi-color observations of the spiral galaxy M33 were obtained in the BATC photometric system which has a custom designed set of 15 intermediate-band filters to do spectrophotometry for preselected 1 deg^2 regions of the northern sky. The telescope used is the 60/90 cm f/3 Schmidt Telescope of Beijing Astronomical Observatory (BAO), located at the Xinglong station. A Ford Aerospace 2048×2048 CCD camera with $15 \mu\text{m}$ pixel size is mounted at the Schmidt focus of the telescope. The field of view of the CCD is $58' \times 58'$ with a pixel scale of $1''.7$.

The multi-color BATC filter system includes 15 intermediate-band filters, covering the total optical wavelength range from 3000 to 10000\AA (see Fan et al. 1996). The filters were specifically designed to avoid contamination from the brightest and most variable night sky emission lines. A full description of the BAO Schmidt telescope, CCD, data-taking system, and definition of the BATC filter systems are detailed elsewhere (Fan et al. 1996; Zheng et al. 1999). The images of M33 covering the whole optical body of M33 were accumulated in 13 intermediate band filters with a total exposure time of about 38 hours from September 23, 1995 to August 28, 2000. The CCD images are centered at R.A. = $01^{\text{h}}33^{\text{m}}50^{\text{s}}.58$ and decl. = $30^{\circ}39'08''.4$ (J2000). The dome flat-field images were taken by using a diffuse plate in front of the correcting plate of the Schmidt telescope. For flux calibration, the Oke-Gunn primary flux standard stars HD 19445, HD 84937, BD +26°2606, and BD +17°4708 were observed during photometric nights (see details from Yan et al. 1999; Zhou et al. 2001). The parameters of the filters and the statistics of the observations are given in Table 1.

2.3. Image Data Reduction

The data were reduced with standard procedures, including bias subtraction and flat-fielding of the CCD images, with an automatic data reduction software named PIPELINE I developed for the BATC multi-color sky survey (Fan et al. 1996; Zheng et al. 1999). The flat-fielded images of each color were combined by integer pixel shifting. The cosmic rays and bad pixels were corrected by comparison of multiple images during combination. The images were re-centered and position-calibrated using the *HST* Guide Star Catalog. The absolute flux of intermediate-band filter images was calibrated using observations of standard stars. Fluxes as observed through the BATC filters for the Oke-Gunn stars were derived by convolving the SEDs of these stars with the measured BATC filter transmission functions (Fan et al. 1996). *Column 6* in Table 1 gives the zero point error, in magnitude, for the standard stars in each filter. The formal errors we obtain for these stars in the 13 BATC filters are $\lesssim 0.02 \text{ mag}$. This indicates that we can define the standard BATC system to an accuracy of $\lesssim 0.02 \text{ mag}$.

2.4. Integrated Photometry

For each globular cluster candidate, the PHOT routine in DAOPHOT (Stetson 1987) was used to obtain magnitudes. To avoid contamination from nearby objects, a smaller aperture of $6''.8$, which corresponds to a diameter of 4 pixels in Ford CCDs, was adopted. Aperture corrections were computed using isolated stars. The spectral energy distributions (SEDs) in 13 BATC filters for 37 star cluster candidates were obtained and are listed in Table 3. For the other 14 candidates, the SEDs can be found in Ma et al. (2001, 2002a, 2002b). Table 3 contains the following information: Column (1) is cluster number that is taken from Mochejska et al. (1998). Column (2) to Column (14) show the magnitudes in different bands. Second row for each globular cluster candidate is the uncertainties of the magnitude in the corresponding bands. The uncertainties for each filter are taken from by DAOPHOT.

2.5. Comparison with Previous Photometry

Using the Landolt standards, Zhou et al. (2002) presented the relationships between the BATC intermediate-band system and *UBVRI* broadband system from the catalogs of Landolt (1983, 1992) and Galadí-Enríquez, Trullols, & Jordi (2000). We show the coefficients of two relationships in equations (1) and (2).

$$m_B = m_{04} + (0.2218 \pm 0.033)(m_{03} - m_{05}) + 0.0741 \pm 0.033, \quad (1)$$

$$m_V = m_{07} + (0.3233 \pm 0.019)(m_{06} - m_{08}) + 0.0590 \pm 0.010. \quad (2)$$

Using equations (1) and (2), we transformed the magnitudes of 51 globular cluster candidates in BATC03, BATC04 and BATC05 bands to ones in the *B* band, and in BATC06, BATC07 and BATC08 bands to ones in *V* band. For candidates 23 and 30, we change m_{05} to m_{04} because of the strong emission in BATC05 band. Figure 2 plots the comparison of *V* (BATC) and (*B*–*V*) (BATC) photometry with previously published measurements (Mochejska et al. 1998). In this figure, our magnitudes/colors are on the x-axis, the difference between our and Mochejska et al. (1998) magnitudes/colors are on the y-axis. In Figure 2, we did not plot the color of candidate 2 because of its large value ($B - V = 2.50$) by Mochejska et al. (1998). Table 4 also shows this comparison. The mean *V* magnitude and color differences (this paper – the paper (of Mochejska et al. 1998)) are $\langle \Delta V \rangle = -0.078 \pm 0.025$ and $\langle \Delta(B - V) \rangle = -0.150 \pm 0.019$ (not including candidate 2), respectively. The uncertainties in *B* (BATC) and *V* (BATC) have been added linearly, i.e. $\sigma_B = \sigma_{04} + 0.2218(\sigma_{03} + \sigma_{05})$, and $\sigma_V = \sigma_{07} + 0.3233(\sigma_{06} + \sigma_{08})$, to reflect the error in the three filter measurements. For the colors, we added the errors in quadrature, i.e. $\sigma_{(B-V)} = (\sigma_B^2 + \sigma_V^2)^{1/2}$. From Figure 2 and Table 4, it can be seen that there is good agreement in the photometric measurements, although there exists a error in color.

3. DATABASES OF SIMPLE STELLAR POPULATIONS

Since the pioneering work of Tinsley (1972) and Searle, Sargent, & Bagnuolo (1973), evolutionary population synthesis has become a standard technique to study the stellar populations of galaxies. This technique benefits from the improvement in the theory of the chemical evolution of galaxies, star formation, stellar evolution and atmospheres, and of the development of synthesis algorithms and the availability of various evolutionary synthesis models. A comprehensive compilation of such models was presented by Leitherer et al. (1996) and Kennicutt (1998). More widely used models are those from the Padova and Geneva group (e.g. Schaerer & de Koter 1997; Schaerer & Vacca 1998; Bressan et al. 1996; Chiosi et al. 1998), GISSEL96 (Charlot & Bruzual 1991; Bruzual & Charlot 1993, hereafter BC93; BC96), PEGASE (Fioc & Rocca-Volmerange 1997) and STARBURST99 (Leitherer et al. 1999).

A simple stellar population (SSP) is defined as a single generation of coeval stars with fixed parameters such as metallicity, initial mass function, etc. (Buzzoni 1997). SSPs are the basic building blocks of synthetic spectra of galaxies that can be used to infer the formation and subsequent evolution of the parent galaxies (Jablonka et al. 1996). They are modeled by a collection of stellar evolutionary tracks with different masses and initial chemical compositions, supplemented with a library of stellar spectra for stars at different evolutionary stages in evolution synthesis models. In order to study the integrated properties of star clusters in M33, as the first step, we use the SSPs of Galaxy Isochrone Synthesis Spectra Evolution Library (hereafter GSSP; BC96) because they are simple and reasonably well understood.

3.1. SED of GSSPs

Charlot & Bruzual (1991) developed a model of stellar population synthesis. In this model, the population synthesis method can be used to determine accurately the distribution of stars in the theoretical color-magnitude diagram for any stellar systems. BC93 presented “isochrone synthesis” as a natural and

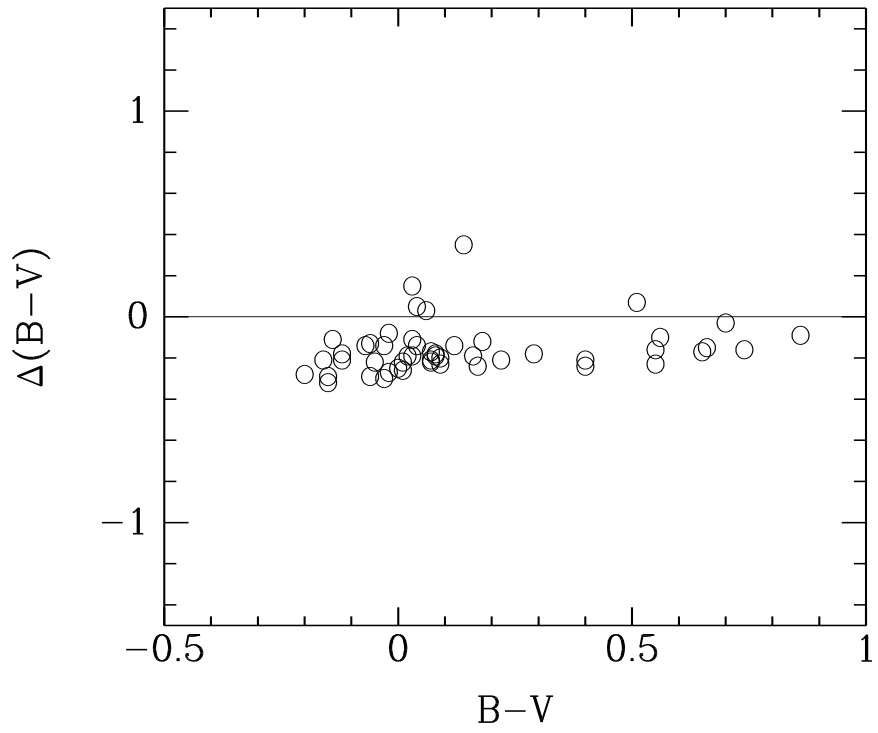
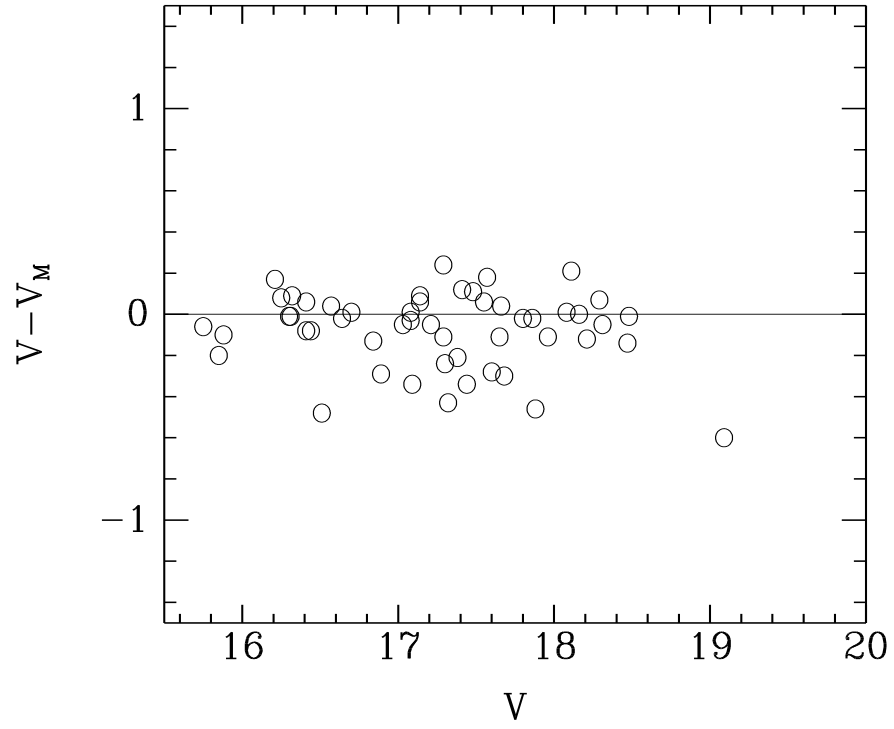


Fig. 2.— Comparison of cluster photometry with previous measurements

reliable approach to model the evolution of stellar populations in star clusters and galaxies. With this isochrone synthesis algorithm, BC93 computed the spectral energy distributions of stellar populations with solar metallicity. BC96 improved BC93 evolutionary population synthesis models. The updated version provides the evolution of the spectrophotometric properties for a wide range of stellar metallicity, which are $Z = 0.0004, 0.004, 0.008, 0.02, 0.05, \text{ and } 0.1$ (see Ma et al. 2001).

3.2. Integrated Colors of GSSPs

Using the multi-color photometry, Kong et al. (2000) have studied the relative chemical abundance, age, and reddening distributions for different components of M81. They obtained the best-fit age and reddening values by minimizing the difference between the observed colors and the predicted values of the theoretical stellar population synthesis models of BC96. To determine the distributions of age for the globular cluster candidates in this paper, we follow the method of Kong et al. (2000). Since the observational data are integrated luminosity, we need to convolve the SED of GSSP with BATC filter profiles to obtain the optical and near-infrared integrated luminosity for comparisons (Kong et al. 2000). The integrated luminosity $L_{\lambda_i}(t, Z)$ of the i th BATC filter can be calculated as

$$L_{\lambda_i}(t, Z) = \frac{\int F_{\lambda}(t, Z)\varphi_i(\lambda)d\lambda}{\int \varphi_i(\lambda)d\lambda}, \quad (3)$$

where $F_{\lambda}(t, Z)$ is the spectral energy distribution of the GSSP of metallicity Z at age t , $\varphi_i(\lambda)$ is the response functions of the i th filter of the BATC filter system ($i = 3, 4, \dots, 15$), respectively. To avoid using distance dependent parameters, we calculate the integrated colors of a GSSP relative to the BATC filter BATC08 ($\lambda = 6075\text{\AA}$):

$$C_{\lambda_i}(t, Z) = L_{\lambda_i}(t, Z)/L_{6075}(t, Z). \quad (4)$$

As a result, we obtain intermediate-band colors for 6 metallicities from $Z = 0.0004$ to $Z = 0.1$.

4. RESULTS

4.1. Cluster Ages

Integrated colors of star clusters depend mostly on age, with a secondary dependence on metallicity. In order to obtain intrinsic colors of 37 globular cluster candidates and hence accurate ages, the photometric measurements must be dereddened. As Chandar, Bianchi, & Ford (2001) did, we adopted $E_{(B-V)} = 0.10$. Besides, we adopted the extinction curve presented by Zombeck (1990). An extinction correction $A_{\lambda} = R_{\lambda}E(B - V)$ was applied; here R_{λ} is obtained by interpolating using the data of Zombeck (1990).

Since we model the stellar populations of the star clusters by SSPs, the intrinsic colors for each star cluster are determined by two parameters: age, and metallicity. We will determine the ages and best-fitted models of metallicity for these star clusters simultaneously by a least-squares method. The age and best-fitted model of metallicity are found by minimizing the difference between the intrinsic and integrated colors of GSSP:

$$R^2(n, t, Z) = \sum_{i=3}^{15} [C_{\lambda_i}^{\text{intr}}(n) - C_{\lambda_i}^{\text{ssp}}(t, Z)]^2, \quad (5)$$

where $C_{\lambda_i}^{\text{ssp}}(t, Z)$ represents the integrated color in the i th filter of a SSP with age t and metallicity Z , and $C_{\lambda_i}^{\text{intr}}(n)$ is the intrinsic integrated color for n th star cluster. Using the stellar evolutionary models (Bertelli et al. 1994) and published line indices of 22 M33 older clusters, Chandar, Bianchi, & Ford (1999b) narrowed

the range of cluster metallicities (Z) to be from ~ 0.0002 to 0.03 . So, we only select the models of three metallicities, 0.0004 , 0.004 and 0.02 of GSSP.

Figure 3 shows the map of the best fit integrated SSP colors (thick line) to the intrinsic integrated colors (filled circles) for 37 globular cluster candidates. Table 4 presents the best-fitted models of metallicities and ages for 37 globular cluster candidates. We also list the age estimates for the other 14 cluster candidates in Table 4. The details about these candidates can be found in Me et al. (2001, 2002a, 2002b). From Figure 3, we can see that clusters 23 and 30 have strong emission lines. In the process of fitting, we did not use the strong emission lines.

Figure 4 presents a histogram of ages for the 51 globular cluster candidates. The results show that, in general, M33 globular clusters have been forming continuously, with ages of $\sim 4 \times 10^6 - 10^{10}$ years, and half candidates are younger than 10^8 . There exist three groups of clusters that formed with three metallicities, $Z = 0.02, 0.004$, and 0.0004 . For different metallicities, the distribution of cluster ages is a little different, too. For $Z = 0.02$, the ages of most clusters are younger than $\sim 10^7$ years. For $Z = 0.004, 0.0004$, the clusters formed from $\sim 4 \times 10^6 - 10^{10}$ years.

In this section, we estimate the ages of 37 globular cluster candidates in M33 by comparing the photometry of each object with the theoretical stellar population synthesis models for different values of metallicity. However, for clusters older than several 10^8 years, the age/metallicity degeneracy becomes pronounced. In this case, we only mean that for some metallicity, the intrinsic integrated color of a cluster provides the best fit to the integrated color of a SSP at some age. The uncertainties in the age estimated arising from photometric uncertainties have typical values 0.2 (in log years).

4.2. Comparison with Previous Results

By comparing the photometric measurements to integrated colors from theoretical models by Bertelli et al. (1994), Chandar et al. (1999b, 2002) estimated ages for 35 globular cluster candidates in common. Figure 5 plots the comparison of distribution of age with previous results (Chandar et al. 1999b, 2002). Table 6 lists this comparison. In order to test whether our results are consistent with Chandar et al. (1999b, 2002), we provide the Kolmogorov-Smirnov Test. The results are that the maximum value of the absolute difference is 0.48 , and the significance level probability is 100.00 per cent.

5. SUMMARY AND DISCUSSION

In this paper, we have, for the first time, obtained the SEDs of 37 globular cluster candidates of M33 in 13 intermediate colors with the BAO 60/90 cm Schmidt telescope. Below, we summarize our main conclusions.

1. Using the images obtained with the Beijing Astronomical Observatory 60/90 cm Schmidt Telescope in 13 intermediate-band filters from 3800 to 10000\AA , we obtained the spectral energy distributions (SEDs) of 37 globular cluster candidates that were detected by Mochejska et al. (1998).
2. By comparing the integrated photometric measurements with theoretical stellar population synthesis models, we find that clusters formed continuously in M33 from $\sim 4 \times 10^6 - 10^{10}$ years. The results also show that, half of the candidates are younger than 10^8 years.

As we know, integrated colors of star clusters depend mostly on age, with a secondary dependence on chemical composition. So, we can estimate ages of clusters, but cannot determine metallicities of clusters with precision. As Chandar, Bianchi, & Ford (1999b, 1999c) did, we also estimated the ages of our sample clusters by comparing the photometry of each object with models for different values of metallicity. Although we presented the metallicity of each cluster in Table 4, we only mean that, for this metallicity,

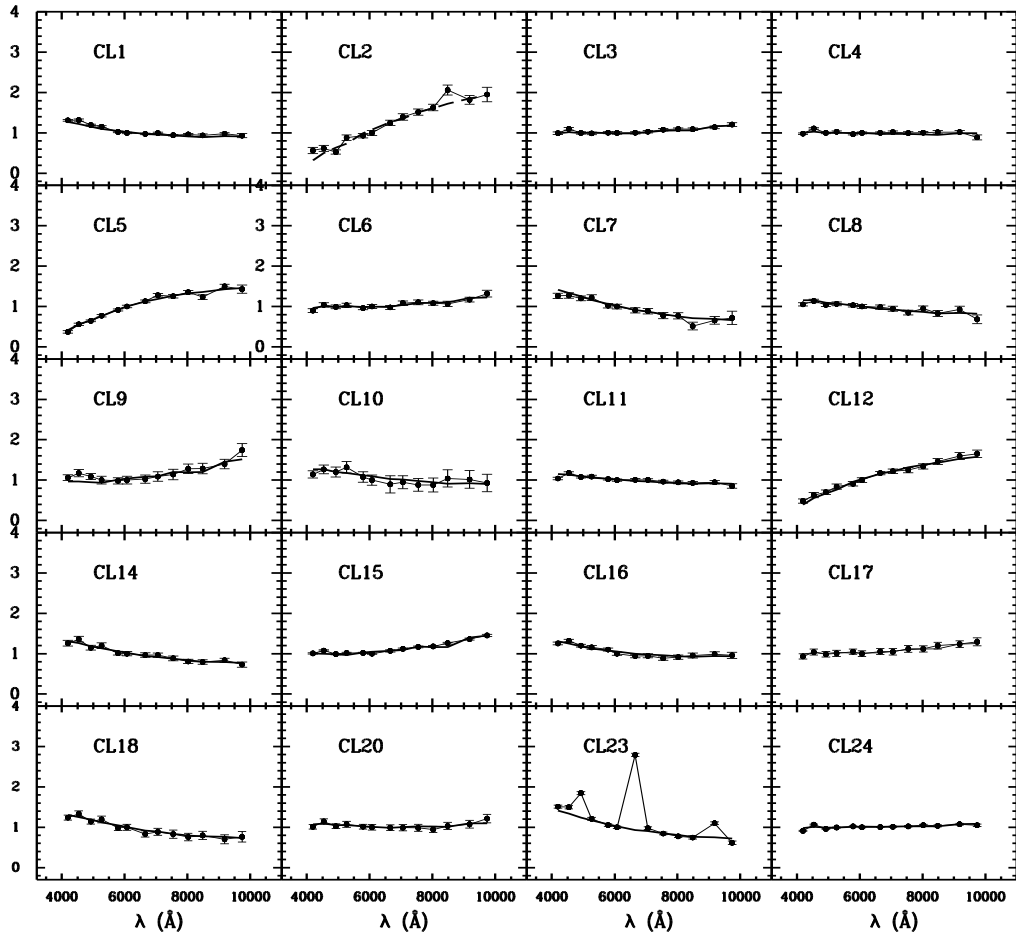


Fig. 3.— Map of the best fit of the integrated color of a SSP with intrinsic integrated color for 37 globular clusters. Thick line represents the integrated color of a SSP, and filled circle represents the intrinsic integrated color of a star cluster.

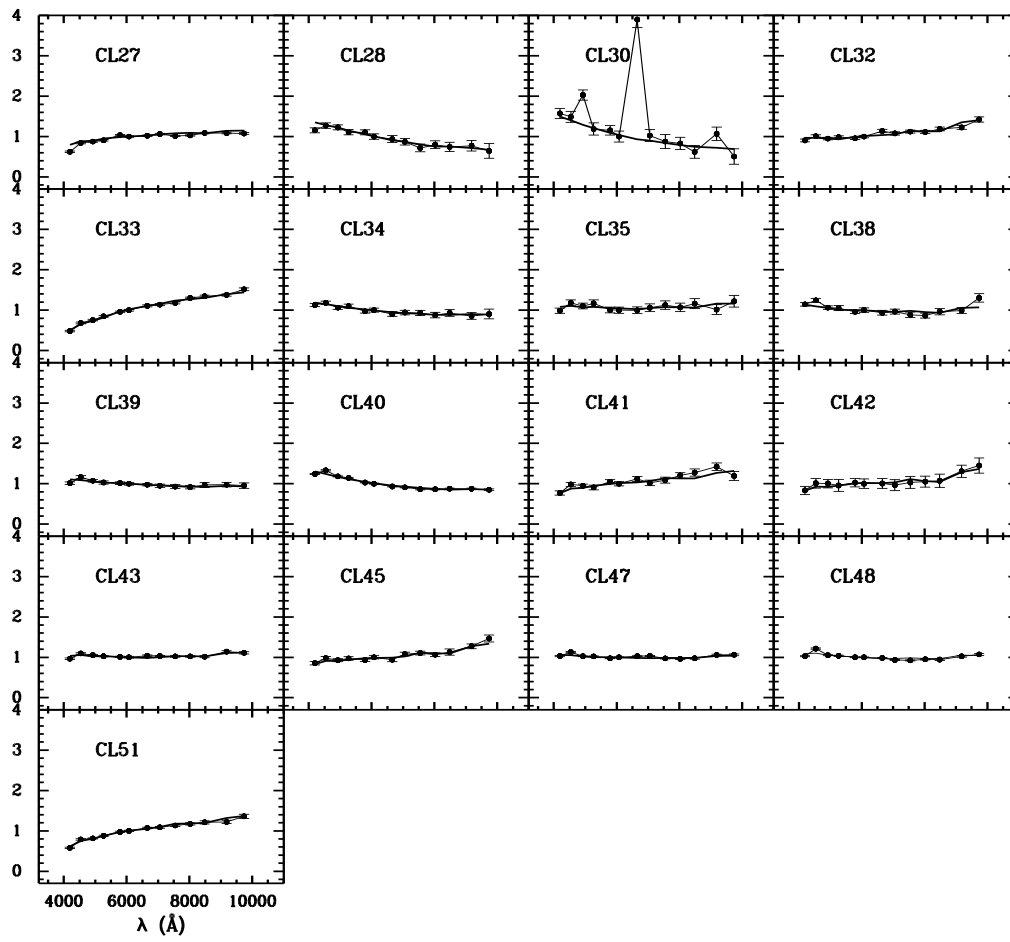


Fig. 3.— Continued

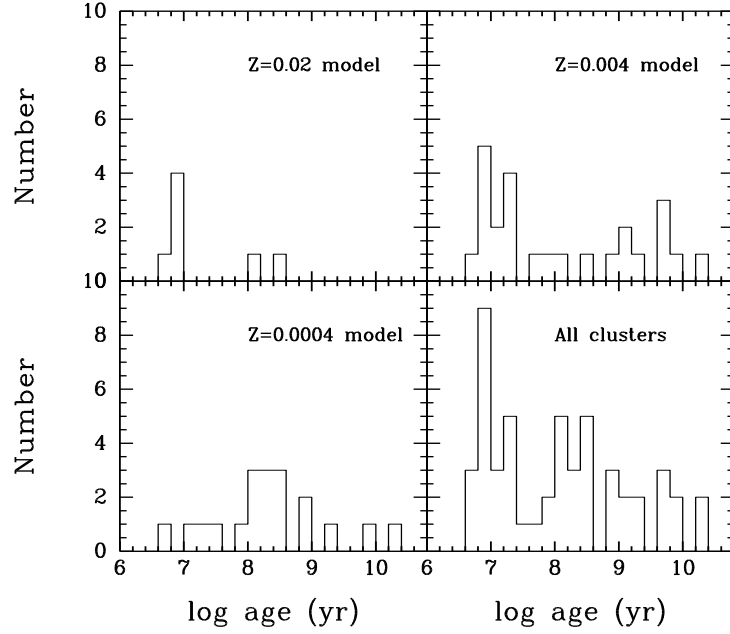


Fig. 4.— Histogram of ages for 51 globular cluster candidates

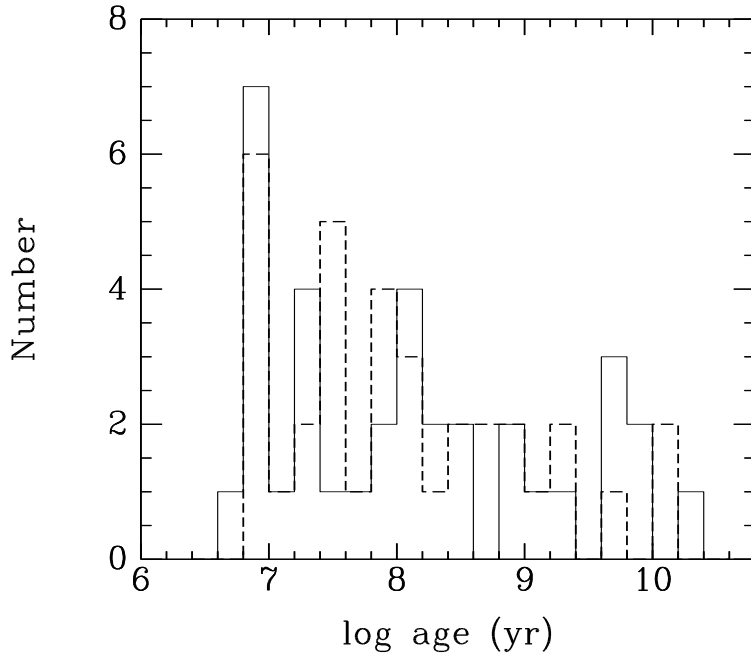


Fig. 5.— Comparison of distribution of age. The solid histogram gives the age estimates in this paper and the dashed histogram shows the results of Chandar et al. (1999b, 2002).

the intrinsic integrated color of each cluster provides the best fit to the integrated color of a SSP.

We would like to thank the anonymous referee for his/her insightful comments and suggestions that improved this paper. We are grateful to the Padova group for providing us with a set of theoretical isochrones and SSPs. We also thank G. Bruzual and S. Charlot for sending us their latest calculations of SSPs and for explanations of their code. The BATC Survey is supported by the Chinese Academy of Sciences, the Chinese National Natural Science Foundation and the Chinese State Committee of Sciences and Technology. The project is also supported in part by the National Science Foundation (grant INT 93-01805) and by Arizona State University, the University of Arizona and Western Connecticut State University.

REFERENCES

- Bertelli, G., Bressan, A., Chiosi, C., Fagotto, F., & Nasi, E. 1994, *A&AS*, 106, 275
- Bressan, A., Chiosi, C., & Tantalò, R. 1996, *A&A*, 311, 425
- Bruzual, G., & Charlot, S. 1993, *ApJ*, 405, 538
- Buzzoni, A. 1997, in *IAU Symp. 183, Cosmological Parameters and Evolution of the Universe*, ed. K. Sato (Dordrecht: Kluwer), 18
- Chandar, R., Bianchi, L., & Ford, H. C. 1999a, *ApJS*, 122, 431
- Chandar, R., Bianchi, L., & Ford, H. C. 1999b, *ApJ*, 517, 668
- Chandar, R., Bianchi, L., Ford, H. C., & Salasnich, B. 1999c, *PASP*, 111, 794
- Chandar, R., Bianchi, L., & Ford, H. C. 2001, *A&A*, 366, 498
- Charlot, S., & Bruzual, G. 1991, *ApJ*, 367, 126
- Chiosi, C., Bressan, A., Portinari, L., & Tantalò, R. 1998, *A&A*, 339, 355
- Christian, C. A., & Schommer, R. A. 1982, *ApJS*, 49, 405
- Christian, C. A., & Schommer, R. A. 1983, *ApJ*, 275, 92
- Christian, C. A., & Schommer, R. A. 1988, *AJ*, 95, 704
- Ciani, A., D’Odorico, S., & Benvenuti, P. 1984, *A&A*, 137, 223
- Fan, X., et al. 1996, *AJ*, 112, 628
- Fioc, M., & Rocca-Volmerange, B. 1997, *A&A*, 326, 950
- Freedman, W. L., Wilson, C. D., & Madore, B. F. 1991, *ApJ*, 372, 455
- Galadí-Enríquez, D., Trullols, E., & Jordi, C. 2000, *A&AS*, 146, 169
- Hiltner, W. A. 1960, *ApJ*, 131, 163
- Jablonka, P., Bica, E., Pelat, D., & Alloin, D. 1996, *A&A*, 307, 385
- Kaluzny, J., Stanek, K. Z., Krockenberger, M., Sasselov, D., Tonry, J. L., & Mateo, M. 1998, *AJ*, 115, 1016
- Kennicutt, R. C. 1998, *A&A Rev.*, 36, 189
- Kong, X., et al. 2000, *AJ*, 119, 2745

- Kron, G. E., & Mayall, N. U. 1960, *AJ*, 65, 581
- Landolt, A. U. 1983, *AJ*, 88, 439
- Landolt, A. U. 1992, *AJ*, 104, 340
- Leitherer, C., et al. 1996, *PASP*, 108, 996
- Leitherer, C., et al. 1999, *ApJS*, 123, 3
- Ma, J., Zhou, X., Kong, X., Wu, H., Chen, J., Jiang, Z., Zhu, J., & Xue, S. 2001, *AJ*, 122, 1796
- Ma, J., Zhou, X., Chen, J., Wu, H., Jiang, Z., Xue, S., & Zhu, J. 2002a, *A&A*, 385, 404
- Ma, J., Zhou, X., Chen, J., Wu, H., Jiang, Z., Xue, S., & Zhu, J. 2002b, *AJ*, 123, 3141
- Melnick, J., & D’Odorico, S. 1978, *A&AS*, 34, 249
- Mochejska, B. J., Kaluzny, J., Krockenberger, M., Sasselov, D. D., & Stanek, K. Z. 1998, *Acta Astron.*, 48, 455
- Sarajedini, A. A., Geisler, D., Harding, P., & Schommer, R. 1998, *ApJ*, 508, L37
- Schaerer, D., & de Koter, A. 1997, *A&A*, 322, 598
- Schaerer, D., & Vacca, W. D. 1998, *ApJ*, 497, 618
- Schmidt, A. A., Bica, E., & Alloin, D. 1990, *MNRAS*, 243, 620
- Searle, L., Sargent, W. L. W., & Bagnuolo, W. G. 1973, *ApJ*, 179, 427
- Stanek, K. Z., Kaluzny, J., Krockenberger, M., Sasselov, D. D., Tonry, J. L., & Mateo, M. 1998, *AJ*, 115, 1894
- Stetson, P. B. 1987, *PASP*, 99, 191
- Tinsley, B. M. 1972, *A&A*, 20, 382
- Yan, H. J., et al. 2002, *PASP*, 112, 691
- Zheng, Z. Y., et al. 1999, *AJ*, 117, 2757
- Zhou, X., Jiang, Z.-J., Xue, S.-J., Wu, H., Ma, J., & Chen, J.-S. 2001, *Chinese Astron. Astrophys.*, 1, 372
- Zhou, X., et al. 2002, *A&A*, in press
- Zombeck, M. V. 1990, *Handbook of Space Astronomy and Astrophysics* (2nd. ed; Cambridge: Cambridge Univ. Press) p. 104

Table 1: Parameters of the BATC filters and statistics of observations

No.	Name	cw ^a (Å)	Exp. (hr)	N.img ^b	rms ^c
1	BATC03	4210	00:55	04	0.024
2	BATC04	4546	01:05	04	0.023
3	BATC05	4872	03:55	19	0.017
4	BATC06	5250	03:19	15	0.006
5	BATC07	5785	04:38	17	0.011
6	BATC08	6075	01:26	08	0.016
7	BATC09	6710	01:09	08	0.006
8	BATC10	7010	01:41	08	0.005
9	BATC11	7530	02:07	10	0.017
10	BATC12	8000	03:00	11	0.003
11	BATC13	8510	03:15	11	0.005
12	BATC14	9170	05:45	25	0.011
13	BATC15	9720	06:00	26	0.009

^aCentral wavelength for each BATC filter

^bImage numbers for each BATC filter

^cZero point error, in magnitude, for each filter as obtained from the standard stars

Table 2: Comparison of common clusters in different studies

MKSS98	MD78	CS82	CBF99 & CBF01
4	10
11	U11
13	44*
19	47*
20	U94
21	24	U49*	61
22	25	H38*	104
24	27
25	49*
26	H14	33*
28	U75
29	28*
31	R14*	98
36	R12*	116
37	141*
38	35	H30
39	39	U62
41	38	U83
42	41	U78
44	42	U82	55*
45	36	H33
46	U79	155*
49	35*
50	U91	58*
51	45	H21

Table 3: SEDs of 37 globular cluster candidates

No.	03	04	05	06	07	08	09	10	11	12	13	14	15
(1)	(2)	(3)	(4)	(5)	(6)	(7)	(8)	(9)	(10)	(11)	(12)	(13)	(14)
1	17.153	17.116	17.194	17.191	17.271	17.287	17.284	17.251	17.290	17.247	17.258	17.190	17.232
	0.019	0.021	0.019	0.024	0.020	0.022	0.019	0.025	0.024	0.024	0.043	0.032	0.061
2	19.660	19.533	19.676	19.079	18.966	18.881	18.610	18.480	18.369	18.272	17.995	18.111	18.024
	0.151	0.129	0.112	0.083	0.064	0.066	0.055	0.062	0.055	0.054	0.065	0.065	0.099
3	17.108	16.968	17.042	17.014	16.945	16.941	16.906	16.868	16.797	16.761	16.745	16.677	16.606
	0.036	0.034	0.031	0.034	0.027	0.030	0.031	0.031	0.031	0.030	0.033	0.032	0.042
4	17.476	17.313	17.396	17.326	17.340	17.297	17.265	17.235	17.240	17.211	17.179	17.154	17.295
	0.022	0.021	0.021	0.024	0.022	0.024	0.027	0.031	0.038	0.037	0.047	0.045	0.074
5	19.174	18.700	18.515	18.279	18.046	17.939	17.776	17.631	17.633	17.530	17.612	17.380	17.421
	0.084	0.051	0.037	0.043	0.031	0.034	0.032	0.036	0.037	0.035	0.050	0.038	0.076
6	17.593	17.404	17.429	17.346	17.371	17.319	17.313	17.191	17.152	17.153	17.152	17.027	16.888
	0.055	0.053	0.050	0.055	0.046	0.054	0.055	0.056	0.056	0.050	0.066	0.055	0.069
7	18.219	18.181	18.214	18.158	18.299	18.313	18.390	18.405	18.528	18.517	18.933	18.651	18.542
	0.054	0.058	0.053	0.064	0.058	0.065	0.075	0.082	0.106	0.108	0.205	0.159	0.248
8	18.030	17.916	17.981	17.916	17.901	17.925	17.911	17.946	18.041	17.901	18.028	17.888	18.207
	0.042	0.042	0.041	0.050	0.046	0.054	0.057	0.070	0.077	0.072	0.099	0.095	0.168
9	17.865	17.727	17.779	17.829	17.799	17.769	17.713	17.638	17.568	17.422	17.396	17.287	17.036
	0.072	0.084	0.074	0.106	0.084	0.106	0.106	0.117	0.124	0.101	0.108	0.091	0.101
10	18.580	18.439	18.465	18.325	18.494	18.563	18.654	18.581	18.641	18.623	18.420	18.426	18.514
	0.088	0.093	0.110	0.116	0.132	0.136	0.256	0.184	0.196	0.212	0.222	0.233	0.251
11	16.928	16.765	16.831	16.780	16.795	16.811	16.775	16.766	16.792	16.795	16.790	16.752	16.854
	0.031	0.029	0.027	0.031	0.025	0.029	0.034	0.033	0.038	0.040	0.043	0.048	0.070
12	17.993	17.672	17.525	17.289	17.151	17.037	16.833	16.781	16.737	16.640	16.527	16.410	16.361
	0.116	0.114	0.089	0.086	0.064	0.064	0.038	0.051	0.055	0.051	0.056	0.058	0.061
14	16.305	16.192	16.345	16.258	16.391	16.394	16.404	16.394	16.468	16.548	16.546	16.467	16.604
	0.060	0.055	0.054	0.063	0.050	0.056	0.062	0.061	0.074	0.071	0.079	0.066	0.097
15	15.844	15.739	15.802	15.732	15.681	15.691	15.588	15.529	15.463	15.432	15.339	15.238	15.157
	0.018	0.015	0.018	0.016	0.015	0.015	0.027	0.019	0.020	0.019	0.020	0.019	0.020
16	17.061	16.975	17.049	17.050	17.052	17.146	17.180	17.167	17.216	17.164	17.096	17.040	17.063
	0.030	0.031	0.030	0.041	0.035	0.044	0.051	0.056	0.065	0.061	0.070	0.065	0.086
17	16.717	16.569	16.596	16.531	16.438	16.480	16.395	16.391	16.299	16.279	16.183	16.129	16.072
	0.077	0.078	0.075	0.082	0.067	0.077	0.076	0.082	0.082	0.076	0.075	0.074	0.084
18	16.962	16.854	16.991	16.903	17.063	17.035	17.204	17.128	17.177	17.255	17.182	17.298	17.202
	0.055	0.058	0.060	0.074	0.070	0.080	0.103	0.106	0.133	0.132	0.140	0.170	0.185
20	17.189	17.027	17.114	17.024	17.036	17.042	17.024	17.014	16.999	17.023	16.910	16.843	16.702
	0.059	0.060	0.060	0.075	0.064	0.074	0.079	0.085	0.095	0.090	0.095	0.095	0.095
23	16.636	16.617	16.358	16.778	16.877	16.924	15.780	16.909	17.047	17.124	17.143	16.701	17.321
	0.026	0.028	0.022	0.034	0.029	0.033	0.016	0.035	0.042	0.041	0.058	0.035	0.076
24	16.764	16.563	16.649	16.570	16.490	16.503	16.468	16.450	16.420	16.369	16.366	16.304	16.320
	0.015	0.013	0.013	0.014	0.013	0.014	0.015	0.016	0.020	0.020	0.023	0.024	0.032
27	16.437	16.080	16.005	15.929	15.736	15.763	15.710	15.657	15.688	15.652	15.570	15.554	15.553
	0.035	0.027	0.022	0.021	0.015	0.018	0.020	0.018	0.018	0.016	0.018	0.020	0.022
28	17.920	17.784	17.795	17.867	17.818	17.916	17.956	18.028	18.215	18.079	18.138	18.074	18.264
	0.058	0.058	0.055	0.064	0.061	0.071	0.102	0.099	0.142	0.130	0.167	0.182	0.311
30	17.084	17.114	16.746	17.289	17.269	17.415	15.908	17.348	17.496	17.539	17.834	17.224	18.026
	0.089	0.101	0.068	0.139	0.110	0.146	0.056	0.160	0.215	0.196	0.280	0.168	0.415
32	17.507	17.360	17.394	17.314	17.298	17.239	17.070	17.117	17.053	17.043	16.953	16.898	16.726
	0.043	0.037	0.035	0.038	0.033	0.033	0.039	0.038	0.038	0.039	0.044	0.039	0.051
33	17.060	16.652	16.515	16.349	16.163	16.107	15.968	15.927	15.868	15.741	15.686	15.640	15.525
	0.045	0.034	0.026	0.031	0.022	0.024	0.022	0.022	0.023	0.020	0.022	0.021	0.024
34	17.545	17.465	17.550	17.474	17.558	17.516	17.597	17.541	17.535	17.578	17.495	17.567	17.495
	0.037	0.041	0.042	0.048	0.048	0.052	0.071	0.064	0.078	0.084	0.094	0.105	0.143

Table 3: Continued

No.	03	04	05	06	07	08	09	10	11	12	13	14	15
(1)	(2)	(3)	(4)	(5)	(6)	(7)	(8)	(9)	(10)	(11)	(12)	(13)	(14)
38	17.551	17.430	17.570	17.543	17.591	17.536	17.580	17.534	17.607	17.614	17.476	17.427	17.118
	0.042	0.043	0.046	0.064	0.051	0.060	0.069	0.070	0.083	0.080	0.087	0.083	0.086
39	17.649	17.469	17.526	17.532	17.498	17.505	17.500	17.519	17.524	17.519	17.437	17.410	17.425
	0.035	0.035	0.033	0.043	0.032	0.037	0.037	0.045	0.052	0.051	0.066	0.060	0.077
40	15.796	15.689	15.789	15.784	15.848	15.870	15.916	15.934	15.967	15.950	15.913	15.895	15.915
	0.011	0.012	0.011	0.013	0.011	0.014	0.014	0.016	0.018	0.017	0.019	0.020	0.028
41	18.172	17.882	17.887	17.894	17.686	17.731	17.577	17.669	17.577	17.448	17.367	17.229	17.409
	0.072	0.056	0.049	0.070	0.049	0.057	0.060	0.071	0.074	0.061	0.077	0.070	0.103
42	18.444	18.204	18.182	18.195	18.069	18.087	18.051	18.082	17.994	17.951	17.910	17.675	17.553
	0.134	0.132	0.114	0.168	0.112	0.128	0.134	0.152	0.157	0.141	0.163	0.126	0.142
43	16.576	16.408	16.420	16.409	16.375	16.377	16.306	16.304	16.292	16.272	16.261	16.114	16.132
	0.019	0.019	0.018	0.018	0.015	0.017	0.021	0.018	0.018	0.018	0.025	0.019	0.028
45	18.239	18.061	18.089	18.000	17.994	17.909	17.946	17.787	17.741	17.761	17.677	17.527	17.364
	0.054	0.047	0.045	0.047	0.041	0.043	0.057	0.047	0.045	0.045	0.073	0.051	0.066
47	16.659	16.531	16.605	16.568	16.570	16.533	16.473	16.458	16.503	16.495	16.459	16.353	16.337
	0.015	0.014	0.012	0.014	0.012	0.013	0.011	0.015	0.015	0.015	0.023	0.021	0.021
48	16.752	16.540	16.667	16.643	16.631	16.622	16.611	16.656	16.649	16.598	16.585	16.476	16.418
	0.016	0.014	0.012	0.014	0.012	0.012	0.013	0.015	0.016	0.017	0.022	0.023	0.025
51	18.066	17.704	17.638	17.515	17.354	17.315	17.210	17.183	17.119	17.062	17.006	16.977	16.851
	0.030	0.022	0.018	0.021	0.017	0.019	0.019	0.022	0.023	0.024	0.038	0.035	0.042

Table 4: Comparison of cluster photometry with previous measurements

No.	V (MKKSS98)	V (BATC)	$B - V$ (MKKSS98)	$B - V$ (BATC)
(1)	(2)	(3)	(4)	(5)
1.....	17.54	17.299 ± 0.035	0.06	-0.118 ± 0.046
2.....	19.69	19.089 ± 0.112	2.50	0.515 ± 0.218
3.....	17.08	17.028 ± 0.048	0.22	0.029 ± 0.068
4.....	17.29	17.408 ± 0.038	0.25	-0.004 ± 0.048
5.....	18.34	18.215 ± 0.056	0.73	0.705 ± 0.096
6.....	17.78	17.439 ± 0.081	0.26	0.076 ± 0.111
7.....	18.36	18.308 ± 0.100	0.17	-0.052 ± 0.129
8.....	18.07	17.957 ± 0.080	0.18	0.044 ± 0.100
9.....	18.34	17.877 ± 0.153	0.07	-0.057 ± 0.192
10.....	18.49	18.476 ± 0.213	0.03	0.063 ± 0.254
11.....	16.97	16.844 ± 0.044	0.21	0.017 ± 0.061
12.....	17.40	17.291 ± 0.112	0.66	0.558 ± 0.195
13.....	17.62	17.661 ± 0.052	0.27	-0.030 ± 0.093
14.....	16.35	16.406 ± 0.088	0.14	-0.149 ± 0.119
15.....	15.81	15.753 ± 0.025	0.28	0.069 ± 0.034
16.....	17.11	17.080 ± 0.062	0.11	-0.028 ± 0.077
17.....	16.99	16.513 ± 0.118	0.35	0.156 ± 0.163
18.....	17.07	17.079 ± 0.120	0.05	-0.158 ± 0.146
19.....	17.75	17.323 ± 0.040	-0.21	0.137 ± 0.072
20.....	17.43	17.089 ± 0.112	-0.12	0.029 ± 0.142
21.....	16.04	16.207 ± 0.019	0.78	0.549 ± 0.032
22.....	17.26	17.208 ± 0.028	0.81	0.664 ± 0.049
23.....	17.18	16.889 ± 0.051	-0.03	-0.136 ± 0.064
24.....	16.53	16.571 ± 0.022	0.29	0.092 ± 0.029
25.....	18.21	18.285 ± 0.092	0.44	0.507 ± 0.213
26.....	17.05	17.141 ± 0.031	0.26	0.118 ± 0.060
27.....	16.05	15.849 ± 0.028	0.61	0.401 ± 0.048
28.....	17.88	17.861 ± 0.105	0.13	0.025 ± 0.134
29.....	16.23	16.322 ± 0.019	0.82	0.652 ± 0.044
30.....	17.05	17.287 ± 0.202	0.06	-0.024 ± 0.244
31.....	16.49	16.414 ± 0.035	0.95	0.857 ± 0.065
32.....	17.59	17.381 ± 0.056	0.27	0.078 ± 0.078
33.....	16.31	16.300 ± 0.040	0.71	0.547 ± 0.064
34.....	17.88	17.603 ± 0.080	0.07	-0.065 ± 0.099
35.....	17.98	17.683 ± 0.130	-0.01	0.038 ± 0.163
36.....	16.32	16.310 ± 0.036	0.90	0.736 ± 0.064
37.....	16.17	16.250 ± 0.074	0.08	-0.202 ± 0.095
38.....	17.76	17.652 ± 0.091	0.17	-0.152 ± 0.110
39.....	17.39	17.566 ± 0.058	0.26	0.005 ± 0.077
40.....	15.98	15.879 ± 0.020	0.09	-0.115 ± 0.026
41.....	17.82	17.798 ± 0.090	0.43	0.222 ± 0.122
42.....	18.16	18.163 ± 0.208	0.41	0.173 ± 0.279
43.....	16.52	16.444 ± 0.026	0.29	0.072 ± 0.038
44.....	17.90	18.112 ± 0.068	0.48	0.295 ± 0.135
45.....	18.07	18.082 ± 0.070	0.32	0.086 ± 0.098
46.....	17.49	17.546 ± 0.055	0.24	0.066 ± 0.069
47.....	16.66	16.640 ± 0.021	0.25	-0.023 ± 0.029
48.....	16.69	16.697 ± 0.020	0.23	-0.064 ± 0.029
49.....	17.08	17.135 ± 0.031	0.23	0.012 ± 0.056
50.....	18.61	18.468 ± 0.101	0.30	0.182 ± 0.190
51.....	17.37	17.478 ± 0.030	0.64	0.395 ± 0.044

Table 5: Age distribution of 51 globular cluster candidates

No. (1)	Metallicity (Z) (2)	Age ([log yr]) (3)	No. (1)	Metallicity (Z) (2)	Age ([log yr]) (3)
1.....	0.00400	7.220	27.....	0.00040	8.957
2.....	0.00400	10.301	28.....	0.00400	6.620
3.....	0.00040	8.407	29.....	0.00040	9.796
4.....	0.00400	7.857	30.....	0.00040	7.179
5.....	0.00040	10.238	31.....	0.00400	9.110
6.....	0.00040	8.507	32.....	0.02000	7.000
7.....	0.02000	6.720	33.....	0.00400	9.207
8.....	0.00040	8.009	34.....	0.00400	7.100
9.....	0.02000	6.960	35.....	0.00040	8.307
10.....	0.00040	8.009	36.....	0.00400	10.000
11.....	0.00400	6.940	37.....	0.00040	6.660
12.....	0.00400	9.628	38.....	0.02000	6.880
13.....	0.00400	7.220	39.....	0.00400	6.960
14.....	0.00040	7.462	40.....	0.00400	7.158
15.....	0.02000	7.000	41.....	0.00400	8.806
16.....	0.00400	7.220	42.....	0.02000	8.556
17.....	0.00040	8.507	43.....	0.00040	8.307
18.....	0.00400	6.820	44.....	0.00040	8.957
19.....	0.02000	8.057	45.....	0.00400	8.556
20.....	0.00040	8.255	46.....	0.00400	6.960
21.....	0.00400	9.600	47.....	0.00400	7.380
22.....	0.00400	9.700	48.....	0.00040	8.057
23.....	0.00040	7.320	49.....	0.00040	7.806
24.....	0.00400	7.699	50.....	0.00400	6.960
25.....	0.00040	9.342	51.....	0.00400	9.009
26.....	0.00400	8.009			

Table 6: Comparison of age estimates for globular cluster candidates with previous measurements

No.	Age ([log yr]) (Chandar et al.)	Age ([log yr]) (This paper)	No.	Age ([log yr]) (Chandar et al.)	Age ([log yr]) (This paper)
(1)	(2)	(3)	(1)	(2)	(3)
1.....	7.4 ± 0.2	7.220	26.....	7.9 ± 0.1	8.009
2.....	> 9.0	10.301	27.....	8.6 ± 0.2	8.957
3.....	8.1 ± 0.3	8.407	29.....	10.2 ± 0.4	9.796
4.....	7.5 ± 0.5	7.857	31.....	10.2 ± 0.2	9.110
7.....	7.0 ± 0.2	6.720	32.....	8.1 ± 0.3	7.000
8.....	7.6 ± 0.2	8.009	34.....	7.4 ± 0.2	7.100
9.....	8.5 ± 0.5	6.960	35.....	7.0 ± 0.2	8.307
11.....	7.2 ± 0.2	6.940	36.....	9.7 ± 0.3	10.000
12.....	9.4 ± 0.2	9.628	38.....	< 7.0	6.880
13.....	< 7.6	7.220	39.....	< 7.0	6.960
14.....	< 7.0	7.462	43.....	8.5 ± 0.2	8.307
16.....	8.0 ± 0.4	7.220	44.....	9.0 ± 0.3	8.957
18.....	< 7.0	6.820	45.....	8.4 ± 0.2	8.556
19.....	< 7.6	8.057	47.....	< 7.5	7.380
21.....	9.2 ± 0.1	9.600	48.....	8.0 ± 0.4	8.057
22.....	9.25 ± 0.15	9.700	49.....	7.7 ± 0.1	7.806
24.....	8.1 ± 0.3	7.320	50.....	8.6 ± 0.3	6.960
25.....	7.9 ± 0.2	9.342			

This figure "majunfig1.gif" is available in "gif" format from:

<http://arxiv.org/ps/astro-ph/0211317v1>